Pertanika J. Sci. & Technol. 25 (S): 49 - 62 (2017)

SCIENCE & TECHNOLOGY

Journal homepage: http://www.pertanika.upm.edu.my/

An Accurate Rejection Model for False Positive Reduction of Mass Localisation in Mammogram

Ashwaq Qasem[1]*, Siti Norul Huda Sheikh Abdullah[1], Shahnorbanun Sahran[1], Rizuana Iqbal Hussain[2] and Fuad Ismail[3]

[1]Pattern Recognition Research Group, Center for Artificial Intelligence Technology(CAIT), Universiti Kebangsaan Malaysia(UKM), 43600, Bangi, Selangor D.E., Malaysia
[2]Department of Radiology, Universiti Kebangsaan Malaysia Medical Centre (UKMMC), 56000, Cheras, Kuala Lumpur, Malaysia
[3]Department of Radiotherapy and Oncology, Universiti Kebangsaan Malaysia Medical Centre (UKMMC), 56000, Cheras, Kuala Lumpur, Malaysia

ABSTRACT

The false positive (FP) is an over-segment result where the noncancerous pixel is segmented as a cancer pixel. The FP rate is considered a challenge in localising masses in mammogram images. Hence, in this article, a rejection model is proposed by using a supervised learning method in mass classification such as support vector machine (SVM). The goal of the rejection model which is based on SVM is the reduction of FP rate in segmenting mammogram through the Chan-Vese method, which is initialised by the marker controller watershed (MCWS) algorithm. The MCWS algorithm is utilised for segmentation of a mammogram image. The segmentation is subsequently refined through the Chan-Vese method, followed by the development of the proposed SVM rejection model with different window size as well as its application in eliminating incorrect segmented nodules. The dataset comprised of 57 nodules and 113 non-nodules and the study successfully proved the effectiveness of the SVM rejection model to decrease the FP rate.

Keywords: Breast cancer, Chan-Vese, Mammogram, MCWS, Rejection model, SVM

ARTICLE INFO

Article history:
Received: 15 August 2016
Accepted: 18 May 2017

E-mail addresses:
eng.ashwaq@gmail.com (Ashwaq Qasem),
snhsabdullah@ukm.edu.my (Siti Norul Huda Sheikh Abdullah),
shahnorbanun@ukm.edu.my (Shahnorbanun Sahran),
rizuana@ppukm.ukm.my (Rizuana Iqbal Hussain),
fuad@ppukm.ukm.my (Fuad Ismail)
*Corresponding Author

ISSN: 0128-7680

INTRODUCTION

Breast cancer is one of the most dangerous and common reproductive cancers that affects mostly women. Breast tumour is an abnormal growth of tissues in the breast and it may be felt as a lump or nipple discharge or change of skin texture around the nipple region. Cancers are abnormal cells that divide uncontrollably

and are able to invade other tissues. Cancer cells have the ability to spread to other parts of the body through the blood and lymphatic systems (Verma, McLeod, & Klevansky, 2010).

Breast cancer is the leading cause of death among middle aged and older women (Mousa, Munib, & Moussa, 2005). According to cancer statistics, breast cancer is the second-most common and the leading cause of cancer deaths among women, second only to lung cancer (The American Cancer Society, 2017). Around 1 in 36 (3%) women die due to breast cancer. It has become a major health issue in the past 50 years, and its incidence has increased in recent years (Althuis, Dozier, Anderson, Devesa, & Brinton, 2005; Jinshan, Rangayyan, Jun, El Naqa, & Yongyi, 2009).The oldest documented cases of breast cancer was in Egypt in 3000 BC. According to this document, one of the cases was treated by cauterisation with a fire drill (Cotlar, Dubose, & Rose, 2003;Vetto, Luoh, & Naik, 2009).

Mammogram became popular due to its ability of detect breast changes up to two years before the specialist or the patient can feel it. This makes the screening method good for early detection which can decrease death rate as well as reduce negative biopsies (Cheng, Cai, Chen, Hu, & Lou, 2003; Eltoukhy, Faye, & Samir, 2010; Pal, Bhowmick, Patel, Pal, & Das, 2008; Rangayyan, Ayres, & Leo, 2007; Tahmasbi, Saki, & Shokouhi, 2011).

Depending on the type of breast tissue, breast mass appears different in a mammogram. While it appears as solid block in dense breast, it appears as a roundish pie in a fatty breast. The mass may be alone or with microcalcifications (Weidong, Shunren, Min, & Huilong, 2005). In some cases, healthy breasts are also diagnosed as suspicious of cancer by the radiologist and unfortunately, unnecessary biopsy is performed on them.

Knowing that there are many possibilities of masses in breast cancer, the detecting these features and localising them are important.

In general, localising the mass is important in computer-aided detection where it searches for the location in the mammogram images and segments it. Cheng et al. (2006) examine the most important approaches used for mass segmentation in mammogram.

Image segmentation using thresholding is the simplest way to isolate the object from its background when the image has a distinct gray level distribution. Segmentation separates the regions by assuming that the region that have gray levels below a specific value, called the threshold, as a background and the region with gray levels higher than the threshold as the object or vice versa. Identifying the threshold value is the key point in this algorithm. By selecting a representable threshold, object extraction will be more accurate. Mostly, image histogram is used to identify the threshold value.

Many researches (AbuBaker, Qahwaji, Aqel, & Saleh, 2005; Dheeba, Albert Singh, & Tamil, 2014; Dominguez & Nandi, 2007; Khan, Khan, & Arora, 2015; Kom, Tiedeu, & Kom, 2007; Shahedi, Amirfattahi, Azar, & Sadri, 2007) have used either single, double, or multi-thresholding approach in mammogram image segmentation. These threshold values are identified through different ways and conditions.

Because of the nonlinearity of intensity in mammogram images, it is difficult to select a perfect threshold value. Another active solution for image segmentation is called Shape-based methods, which can overcome threshold limitation in mammogram segmentation.

In a contour-based method, the level set algorithm is used to localise masses (Ball & Bruce, 2007; Dubey, Hanmandlu, & Gupta, 2010; Kisilev, Walach, Hashoul, Barkan, Ophir, & Alpert, 2015; Liu, Liu, Zhou, & Tang, 2010; Rouhi & Jafari, 2016; Xie, Li, & Ma, 2015).

Dubey, Hanmandlu, and Gupta (2010), Liu, Chen, Liu, Chun, Tang, and Deng, (2011) and Ming, Yingying, and Jianzhong (2011) discussed an integrated method to localise masses in mammograms. They combined the level set and MCWS by using the level set method initialised by MCWS. Another novel approach to reduce the FP rate is by using a hybrid approach, namely region growing and active contour proposed by Xiaoming, Xin, Jun, and Zhilin (2011). Qasem, Abdullah, Sahran, Wook, Hussain, Abdullah, and Ismail (2014) had also used MCWS to initialise level set in active contour but they had tested it on smaller dataset and single fixed window size for FP masses rejection using SVM.

Thus, active contour is the most common approach (Lesniak, Hupse, Blanc, Karssemeijer, & Székely, 2012; Liu et al., 2010; Xiaoming et al., 2011) for mass localisation using mammogram. Earlier studies have shown the level set without reinitialisation produced good results in mass segmentation compared with other state-of-the-art algorithm. However, it still has few limitations in terms of initial contour and over-segmentation and in order to overcome these, a better initial contour and post-segmentation enhancement method is needed. Some studies have used the initial contour obtained by an expert radiologist, which slowed down the segmentation process because of interference, and made the segmentation not fully automated (Shi et al., 2008; Liu et al., 2010). Only a few studies had used a better initialisation algorithm, which is MCWS (Dubey, Hanmandlu, & Gupta, 2010; Liu et al., 2011; Ming, Yingying, & Jianzhong, 2011; Qasem et al., 2014). They showed good result but it still needs enhancements to reduce the FP rate. In addition, most of them did not take FP reduction mechanism into consideration. On the other hand, some researchers used morphological operation to enhance the segmentation algorithm.

A proposed Mass localisation method is discussed in this article. The proposed method is a rejection model based on SVM algorithm used to reduce the FP of the output of the Chan-Vese segmentation algorithm that was initialised by MCWS. The remainder of this article is organised as follows: Section 2 discusses in detail the proposed method while Section 3 examines the results. Section 4 concludes the paper.

MATERIALS AND METHODS

The proposed algorithm consists of three important stages; i) initial segmentation, ii) segmentation using Chan-Vese, and iii) refined segmentation using SVM rejection model. Figure 1 shows the steps taken according to the proposed method. First, the source image is cropped to remove any unnecessary parts in an image. Based on the high dimensionality in digital mammogram images, the image is then resized to speed up the subsequent processes. After completing the pre-processing stage, the SVM rejection model is built to reduce the FP rate. Pre- and post-segmentation enhancement for Chan-Vese level set algorithm is then proposed to localise masse in the mammogram.

A key to achieve a good segmentation result using Chan-Vese is the initial contour. Instead of getting the initial contour from the expert, here, MCWS algorithm is used to obtain the initial

contour as well as to eliminate the noise. This makes the proposed method fully automated and reduces the time of interference. Based on the morphology, watershed was proposed by Digabel and Lantuejoul in 1977. To localise mass in mammogram, Chan-Vese active contour based algorithm was used. Chan-Vese can find and maximise the convergence range as well as treat the topological change. This ensures Chan-Vese performs well in image segmentation.

Rejection Model

Support Vector Machine is a learning machine algorithm expounded by Cortes and Vapnik (1995) at the AT&T Bell Laboratories that strives to address the issues pertaining to a two-group classification. The underlying working principle of this algorithm is to search for the optimal hyperplane that sets positive classes (+1) apart from negative classes (-1).

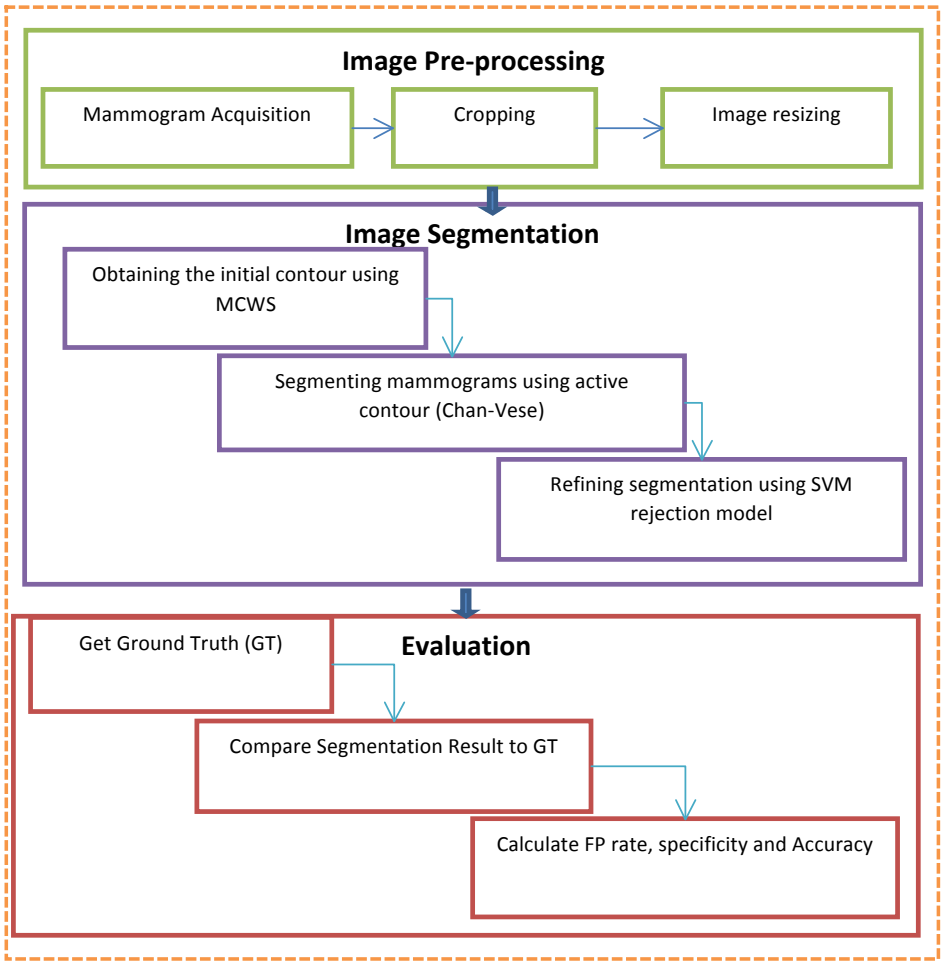

Figure 1. The general steps of the proposed method

In this context, the two classes are the nodules and the non-nodules of breast images, of which the provided training data was used for the SVM to build a model in predicting the target values of the two test data attributes. In this research, the radial basis function (RBF) kernel is employed in complementary with the SVM. The two best parameters, C and γ are prerequisites for the generation of an accurate breast nodule and non-nodule classification by the RBF kernel.

The SVM rejection model has three phases: extracting teacher image, training, and testing. The process diagram is shown in the Figure 2.

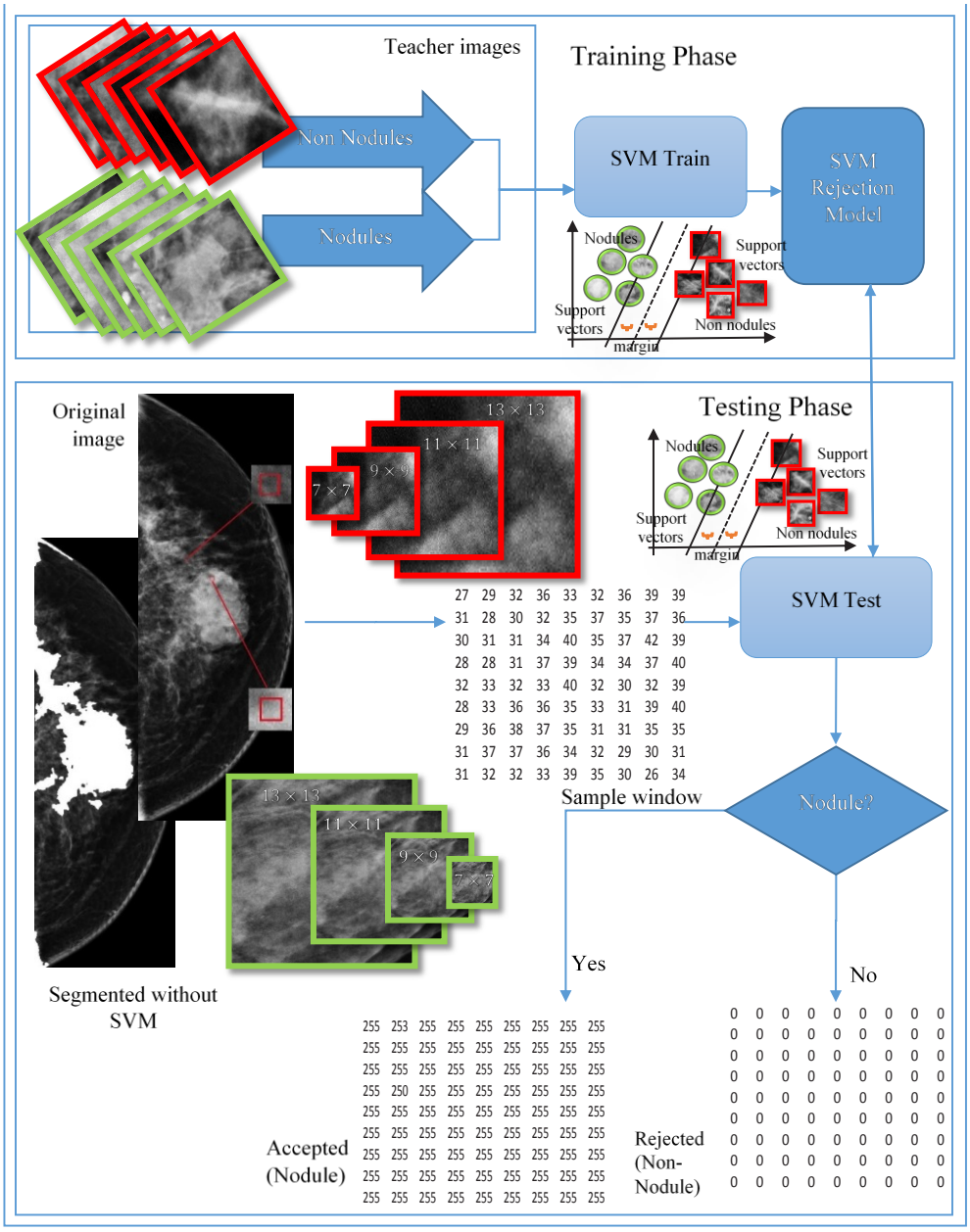

Figure 2. The process diagram of the proposed FP rejection module using SVM method

The grid has been used as a straightforward search on the training data to find the best parameters. The reason for using the grid search instead of other search algorithms is because of its short computation time. Additionally, the grid search can be easily parallelised because it is independent. The search spaces used in this research are $[2^{-5}, 2^{10}]$. It is important to note that this study used the strategy of dividing the data set into two parts of which one is considered unknown. The prediction accuracy obtained from the unknown set will reflect on the classification performance of the independent data set. This procedure is known as cross validation. Its goal is to divide the training set into v subsets of equal size. One subset will be tested using the classifier trained on the remaining subsets. Subsequently, each instance of the training set will be predicted once. Therefore, the cross-validation accuracy is the percentage of data that have been correctly classified.

The training data (teacher images) for the rejection model was manually extracted from the mammogram images by analysing the false positives (FP) and true positives (TP) of the Chan-Vese segmentation result.

After the teacher images were extracted, they were resized using the same factor for the original image. Next, depending on the window size that considered the number of inputs to SVM rejection model, the teacher image was resized. Based on the experiment, either a window size of (7×7) , (9×9) , (11×11) or (13×13) was taken into consideration.

After that, the image was transferred to a vector, and then written into the training data file. This file contained two variables, x and y. The first variable, x is a matrix containing rows of window pixel values for the teacher images. Each row represented one image. The length of the rows depended on the window size. The number of rows in this variable depended on the number of teacher images. The other variable, y is a vector containing the class for each image. The class may be '1' for nodule images or '0' for non-nodule images.

Before proceeding with the SVM rejection training, training data were used to obtain the best values for parameters C, γ. As previously mentioned, the grid search was used as a straightforward search on the training data to obtain these values. Cross validation was also applied to spilt the training data 10-fold into training and testing. Depending on the best accuracy value returned by SVM, the best C and best γ values were chosen. The SVM rejection model was built using the selected C and γ values, and the training dataset. Each row in the training data (x_i) represents an observation, and each column represents features. Class labels (y_i) represent the class label for the corresponding row in the training data.

Table 1
Data set

	Training Data		Testing Data	
	Nodule	Non-nodule	Nodule	Non-nodule
Number of images	11	17	46	96
Total number of images	28	142		

RESULTS

Experiment Setup

About 170 mammogram images were collected from the UKM Medical Centre (HUKM). Table 1 shows training and testing data that have been used in the experiment. The teacher images extracted from the training data based on the segmentation result contained about 35 nodule images and 35 non-nodule images extracted from the training dataset.

The SVM rejection model was run 10 times with a standard deviation of 0.0001, and the results showed the effectiveness of using the rejection model compared with the ground truth.

As mentioned earlier, the grid search was used as a straightforward search on the training data to determine the best parameters C, γ. Table 2 shows values of C, γ using various window sizes (7 × 7), (9 × 9), (11 × 11) and (13 × 13).

Evaluation

The proposed method was evaluated by comparing the segmented images to the ground truth. To show the effectiveness of the proposed method, a comparison was done before and after the rejection model, as shown in Figure 3. This process was performed first by comparing each pixel in the resulting image with the corresponding pixel in the ground truth image. Then, objective evaluation was used to evaluate the method by calculating the confusion matrix as in Table 4, based on the prediction result and the actual ground truth.

Accuracy denotes the proportion of the correct result and it can be calculated as follow:

$$Accuracy(AC) = \frac{TP + TN}{TP + FP + TN + FN} \quad (1)$$

where TP is true positives, TN is true negatives, FP is false positives (type 1 error), and FN is false negatives (type 2 error). In mass localisation, the concept of the confusion matrix in Table 3 represents the correctly segmented nodule and non-nodule with the miss segment. TP and TN are the correctly localised nodule and non-nodule respectively, while FP is the incorrectly segmented non-nodule as a nodule and FN is incorrectly segmented nodule as a non-nodule.

Table 2
C and γ in different window size

Window size		
7 × 7	9.77×10^{-4}	20.898
9 × 9	9.77×10^{-4}	12.642
11 × 11	9.77×10^{-4}	8.462
13 × 13	$3/0518 \times 10^{-5}$	34.2759

Table 3
Confusion matrix

		Result (Predicted)	
		Nodule pixel	Non-Nodule pixel
Ground Truth (Actual)	Nodule Pixel	TP	FN
	Non-Nodule Pixel	FP	TN

Specificity is also known as TN rate and it represents the ability of the method to identify the non-nodule and avoiding false positives.

$$Specificity(SP) = \frac{TN}{TN + FP} \tag{2}$$

Sensitivity which is also known as TP rate or recall represents the ability to identify the nodule and avoid false negatives.

$$Sensitivity(SE) = \frac{TP}{TP + FN} \tag{3}$$

The FP rate shows the non-nodule pixel which is segmented as nodule. It is an over segmented pixel.

$$FP\ rate = \frac{FP}{FP + TN} \tag{4}$$

The FN rate shows the nodule pixel which is segmented as non-nodule. It is the miss segmented pixels.

$$FN\ rate = \frac{FN}{FN + TN} \tag{5}$$

The NRM shows the mismatch between the predicted results and the actual ground truth.

$$Negative\ Rate\ Matric(NRM) = \frac{FP\ rate + FN\ rate}{2} \tag{6}$$

The Effectiveness of Rejection Model

Table 4 and Figure 3 show the quantitative analysis of the results and sample of the result. The effectiveness of the proposed method can be proven by comparing the result before and after using the rejection model. Table 4 shows the FP rate of the proposed rejection model is inversely proportionate to the window size. On the other hand, the specificity rate of the proposed rejection model is linearly proportional to window size.

Table 4
Result

	FP rate	SP	AC	NRM	Over lap
Without the Rejection Model	0.196	0.803	0.803	0.099	0.800
With the Rejection Model (7 × 7) (Qasem et al., 2014)	0.058	0.941	0.938	0.031	0.933
With the Rejection Model (9 × 9)	0.051	0.948	0.944	0.028	0.940
With the Rejection Model (11 × 11)	0.044	0.955	0.950	0.025	0.946
With the Rejection Model (13 × 13)	0.040	0.959	0.954	0.023	0.950

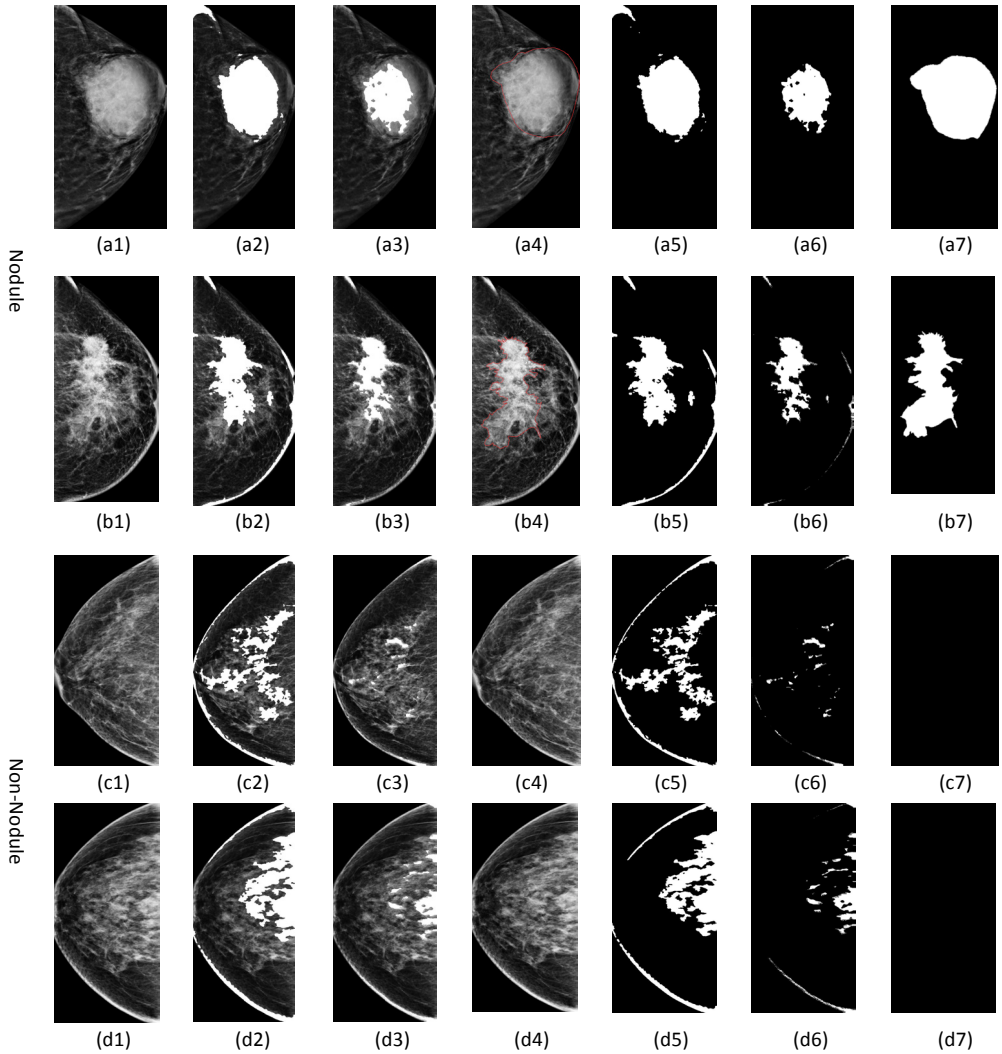

Figure 3. Result before and after using SVM model. (a1, b1, c1 and d1) original non-nodule and nodule images. (a2, b2, c2 and d2) segmentation result without using SVM rejection model, (a3, b3, c3 and d3) segmentation result after reducing the FP rate using SVM rejection model, (a4, b4, c4 and d4) ground truth images, (a5,5, bc5 and d5) binary segmentation result without using SVM rejection model, (a6, b6, c6 and d6) binary segmentation result after reducing the FP rate using SVM rejection model, (a7, b7, c7 and d7) ground truth images.

Expert Evaluation

The result was presented to a medical expert several times. The expert reviewed, evaluated, and accepted both final segmentation results of the proposed method and state of the art technology used.

DISCUSSION

The paper discussed reducing the FP rate based on SVM machine learning. The SVM rejection model was built to reduce the FP rate after segmentation.The proposed method has three steps in the segmentation phase: first, MCWS was used to obtain the initial contour by segmenting the mammogram image. Then, the output of MCWS was used as an initial contour to the Chan-Vese algorithm. Finally, the rejection model based on SVM was used in order to reduce the FP rate. The SVM rejection model has three steps in the following order: extracting teacher images, training the rejection model, and testing the model.

The FP rate reduction by means of SVM machine learning had been put forth wherein the FP rate, upon segmentation, had been reduced by the developed SVM rejection model. The segmentation of the mass in mammogram images as well as the extraction of the initial contour were performed through MCWS, of which the proposed method comprises. The Chan-Vese algorithm is employed as the initial contour to enhance the result of the segmentation. The three steps of the SVM rejection model are as the following sequence: extracting teacher images, training the rejection model, and testing the model.

Credence can be given to the MCWS algorithm in surmounting the challenges associated with the Chan-Vase algorithm. The Chan-Vese algorithm can be made more autonomous and converge faster by using a good initialisation generated by MCWS. Nevertheless, the reliance mammogram segmentation on the divergence and convergence of the intensity value of the image pixels is the constraint factor for this algorithm. The tendency has been towards segmenting the outlier component as part of the contour component, resulting in an incremental FP rate of the selected contour pixels. Accordingly, to overcome this issue, the SVM rejection model is geared towards reducing the FP rate.

T-test was performed to determine the mean difference of two samples, that is, the accuracy before and after using rejection model with the best window size, which is (13 × 13). The T-test was applied to determine if there was a difference before and after applying the rejection model. The hypothesis mean difference of T-test was set to value 0, also named as null hypothesis. That means, assuming that there was no difference in the result whether using the rejection model or not. The alpha was set to value 0.05. The concept of T-test states that if the P value is less than the assumed alpha, the null hypothesis is not correct and there is a difference between the mean of the two samples.

T-Test result shows that the proposed method is considered statistically significant with ($P= 0.00001< 0.05$). Furthermore, the proposed rejection models also showed less standard deviation (0.0001) and yields to stability in its performance.

In general, this proposed method offers alternative decision-making ability and is able to assist the medical expert in giving second opinion on more precise nodule detection. Hence, it reduces FP rate that causes over segmentation.

CONCLUSION

In summary, this proposed method had demonstrated that the SVM rejection process was favourable in reducing FP rate. Based on these findings, it can be assumed that this rejection model would be used. However, further studies are needed to enhance the result.

ACKNOWLEDGMENT

The authors thank the Faculty of Information Science and Technology, Universiti Kebangsaan Malaysia, for providing the facilities and financial support under "ETP-2013-053 diagnostic services nexus for breast cancer". Gratitude is also due to Human Life Advancement Foundation (HLAF) for its financial support. Ethics approval was obtained entitled "FF-338-2012 Breast Cancer Diagnostic Imaging System Using Mammogram and Ultrasound" from UKM Medical Center, Malaysia, for collecting and studying breast cancer patient records.

REFERENCES

AbuBaker, A., Qahwaji, R. S., Aqel, M. J., & Saleh, M. H. (2005). Average Row Thresholding Method for mammogram segmentation. 27th *Annual International Conference of the Engineering in Medicine and Biology Society* (pp. 3288-3291). IEEE - EMBS.

Althuis, M. D., Dozier, J. M., Anderson, W. F., Devesa, S. S., & Brinton, L. A. (2005). Global trends in breast cancer incidence and mortality 1973–1997. *International Journal of Epidemiology, 3*4(2), 405-412.

Ball, J., & Bruce, L. (2007). Digital mammographic computer aided diagnosis (CAD) using adaptive level set segmentation. *Paper presented at the Engineering in Medicine and Biology Society,* 2007. EMBS 2007. 29th Annual International Conference of the IEEE.

Cheng, H., Shi, X., Min, R., Hu, L., Cai, X., & Du, H. (2006). Approaches for automated detection and classification of masses in mammograms. *Pattern Recognition, 3*9(4), 646-668.

Cheng, H. D., Cai, X., Chen, X., Hu, L., & Lou, X. (2003). Computer-aided detection and classification of microcalcifications in mammograms: A survey. *Pattern Recognition, 36*(12), 2967-2991.

Cortes, C., & Vapnik, V. (1995). Support-vector networks. *Machine Learning, 20*(3), 273-297.

Cotlar, A. M., Dubose, J. J., & Rose, D. M. (2003). History of surgery for breast cancer: Radical to the sublime. *Current Surgery, 60*(3), 329-337.

Dheeba, J., Albert S., N., & Tamil S., S. (2014). Computer-aided detection of breast cancer on mammograms: A swarm intelligence optimized wavelet neural network approach. *Journal of Biomedical Informatics, 49*, 45-52.

Dominguez, A. R., & Nandi, A. K. (2007, April). Enhanced multi-level thresholding segmentation and rank based region selection for detection of masses in mammograms. *International Conference on the Acoustics, Speech and Signal Processing (ICASSP)*1, 1-449 IEEE .

Dubey, R. B., Hanmandlu, M., & Gupta, S. K. (2010). A comparison of two methods for the segmentation of masses in the digital mammograms. *Computerized Medical Imaging and Graphics, 34*(3), 185-191.

Eltoukhy, M. M., Faye, I., & Samir, B. B. (2010). Breast cancer diagnosis in digital mammogram using multiscale curvelet transform. *Computerized Medical Imaging and Graphics, 34*(4), 269-276.

Jinshan, T., Rangayyan, R. M., Jun, X., El Naqa, I., & Yongyi, Y. (2009). Computer-aided detection and diagnosis of breast cancer with mammography: Recent advances. *Information Technology in Biomedicine, IEEE Transactions on, 13*(2), 236-251.

Khan, A. A., Khan, M., & Arora, A. S. (2015, July). Automatic detection of malignant neoplasm from mammograms. *In Science and Information Conference (SAI)*, 2015 (pp. 292-297). IEEE.

Kisilev, P., Walach, E., Hashoul, S., Barkan, E., Ophir, B., & Alpert, S. (2015). Semantic description of medical image findings: Structured learning approach.

Kom, G., Tiedeu, A., & Kom, M. (2007). Automated detection of masses in mammograms by local adaptive thresholding. *Computers in Biology and Medicine, 37*(1), 37-48.

Lesniak, J., Hupse, R., Blanc, R., Karssemeijer, N., & Székely, G. (2012). Comparative evaluation of support vector machine classification for computer aided detection of breast masses in mammography. *Physics in Medicine and Biology, 57*(16), 5295.

Liu, J., Chen, J., Liu, X., Chun, L., Tang, J., & Deng, Y. (2011). Mass segmentation using a combined method for cancer detection. *BMC Systems Biology, 5*(Suppl 3), S6.

Liu, X., Liu, J., Zhou, D., & Tang, J. (2010). A benign and malignant mass classification algorithm based on an improved level set segmentation and texture feature analysis. *Paper presented at the Bioinformatics and Biomedical Engineering (iCBBE), 2010 4th International Conference on* (pp. 1-4). IEEE.

Ming, Z., Yingying, C., & Jianzhong, W. (2011, January). An integrated method for breast mass segmentation in digitized mammograms. *3rd International Conference on the Advanced Computer Control (ICACC)* (pp. 214-218). IEEE.

Mousa, R., Munib, Q., & Moussa, A. (2005). Breast cancer diagnosis system based on wavelet analysis and fuzzy-neural. *Expert Systems with Applications, 28*(4), 713-723.

Pal, N. R., Bhowmick, B., Patel, S. K., Pal, S., & Das, J. (2008). A multi-stage neural network aided system for detection of microcalcifications in digitized mammograms. *Neurocomputing, 71*(13–15), 2625-2634.

Qasem, A., Abdullah, S. N. H. S., Sahran, S., Wook, T. S. M. T., Hussain, R. I., Abdullah, N., & Ismail, F. (2014). Breast cancer mass localization based on machine learning. 1*0th International Colloquium on Signal Processing & its Applications (CSPA)* (pp. 31-36). IEEE.

Rangayyan, R. M., Ayres, F. J., & Leo D., J. E. (2007). A review of computer-aided diagnosis of breast cancer: Toward the detection of subtle signs. *Journal of the Franklin Institute, 344*(3–4), 312-348.

Rouhi, R., & Jafari, M. (2016). Classification of benign and malignant breast tumors based on hybrid level set segmentation. *Expert Systems with Applications, 46*, 45-59.

Shahedi, B. K. M., Amirfattahi, R., Azar, F. T., & Sadri, S. (2007, June). Accurate breast region detection in digital mammograms using a local adaptive thresholding method. *Eighth International Workshop on Image Analysis for Multimedia Interactive Services (WIAMIS)*. (pp. 26-26). IEEE.

Shi, J., Sahiner, B., Chan, H., Ge, J., Hadjiiski, L., Helvie, M., Nees, A.,Wu, Y., Wei, J., Zhou, C., Zhang, Y., & Cui, J. (2008). Characterization of mammographic masses based on level set segmentation with new image features and patient information. *Medical Physics 35*(1), 280–90.

Tahmasbi, A., Saki, F., & Shokouhi, S. B. (2011). Classification of benign and malignant masses based on Zernike moments. *Computers in Biology and Medicine, 41*(8), 726-735.

The American Cancer Society. (2017). How common is breast cancer? (Retrieved on date January 22, 2018 from https://www.cancer.org/cancer/breast-cancer/about/how-common-is-breast-cancer.html)

Verma, B., McLeod, P., & Klevansky, A. (2010). Classification of benign and malignant patterns in digital mammograms for the diagnosis of breast cancer. *Expert Systems with Applications, 37*(4), 3344-3351.

Vetto, J. T., Luoh, S. W., & Naik, A. (2009). Breast cancer in premenopausal women. *Current Problems in Surgery, 46*(12), 944-1004.

Weidong, X., Shunren, X., Min, X., & Huilong, D. (2006, January). A model-based algorithm for mass segmentation in mammograms. *27th Annual International Conference of the Engineering in Medicine and Biology Society (*IEEE-EMBS) (pp. 2543-2546). IEEE.

Xiaoming, L., Xin, X., Jun, L., & Zhilin, F. (2011, October). A new automatic method for mass detection in mammography with false positives reduction by supported vector machine. *4th international conference on Biomedical engineering and informatics (BMEI)* (1, 33-37). IEEE.

Xie, W., Li, Y., & Ma, Y. (2015). Breast mass classification in digital mammography based on Extreme learning machine. *Neurocomputing*.